

Single shot NMR on single, dark nuclear spins

G. Waldherr, J. Beck, M. Steiner, P. Neumann,* A. Gali,† F. Jelezko, and J. Wrachtrup
3. Physikalisches Institut, University of Stuttgart, 70550 Stuttgart, Germany

(Dated: July 21, 2022)

The electron and nuclear spins associated with the nitrogen-vacancy (NV) center in diamond are supposed to be building blocks for quantum computing devices and nanometer scale magnetometry operating under ambient conditions. For every such building block precise knowledge of the involved quantum states is crucial. Especially for solid state systems the corresponding Hilbert space can be large. Here, we experimentally show that under usual operating conditions the NV color center exists in an equilibrium of two charge states (i.e. 70% in the usually used negative (NV^-) and 30% in the neutral one (NV^0)). Projective quantum non-demolition measurement of the nitrogen nuclear spin enables the detection even of the additional, optically inactive state. It turns out that the nuclear spin can be coherently driven also in NV^0 . However, its $T_1 \approx 90$ ms and $T_2 \approx 6$ μ s times are much shorter than in NV^- , supposedly because of the dynamic Jahn-Teller effect.

Electron and nuclear spins of the NV color center in diamond are promising candidates for solid state quantum information processing [1–9] and field sensing at nanometer scale under ambient conditions [10, 11]. It consists of a substitutional nitrogen atom next to a lattice vacancy and if negatively charged exhibits an electron spin triplet ground state with very favorable coherence properties [12–14]. Furthermore, electron and nuclear spins can be efficiently initialized and readout optically even at room temperature.

By optically pumping with laser light in the green spectral range the NV^- center is initialized into the $m_S = 0$ spin sublevel of its triplet ($S = 1$) ground state. It is this state that exhibits a higher fluorescence rate than the $m_S \pm 1$ states which is vital for optical spin state detection. In the same time the electronic spin is polarized to a degree far beyond thermal equilibrium which is a necessity for quantum computing and magnetometry. All these features belong to the negative charge state of the NV center which is referred to as “bright state” in the rest of this letter (fig. 3(a)). However, the NV center can also be present in different charge states. Depending on the Fermi level other charge states can be more stable such as the neutral one (NV^0) which is associated with fluorescence with a zero phonon line at 575 nm and a phonon sideband up to 700 nm [15]. It was shown that laser irradiation can induce interconversions between NV^- and NV^0 [16, 17]. Furthermore, recently a long living (150 s) “dark state” was observed [18]. Owing to applications as quantum bit the precise characterization and control of the NV center initial state is crucial.

In this letter we show that quantum non-demolition (QND) measurement of single nitrogen nuclear spins at room temperature can be used to probe different charge states of the NV center. We provide a quantitative analysis of populations in different NV center charge states. It will turn out that next to the negative charge state (bright state) the NV center resides a substantial amount of time in the dark state. Although it is optically inactive it can be detected by the characteristic hyperfine

coupling of the nuclear spin.

The experimental setup consists of a homebuilt room temperature microscope adapted for single spin magnetic resonance. It allows projective read out of a single nuclear spin in a “single shot” as recently discovered [19]. Thus, now we are able to correlate the absolute numbers of attempts to flip a spin and real spin flips. The experiments have been performed on several single, natural abundant NV centers in bulk and nano-diamonds (average size: 50 nm). Figure 1(a) shows Rabi nutations of the ^{14}N nuclear spin ($I = 1$). The vertical axis shows the probability for a spin flip induced by radio frequency (rf). The limited readout and initialization fidelity F reduces the contrast of measurement symmetrically (i.e. full oscillations start at $1 - F^2$ and go up to F^2). Remarkably, the visible oscillations are not symmetric with respect to the 50/50 spin flip probability line indicating that in 30% of all cases the radio frequency does not flip the nuclear spin even for well adjusted π -pulses and high Rabi frequencies. This is because the nuclear spin is out of resonance in the latter cases. We attribute this effect to the NV center being in an unknown state (which might also be another charge state) with a different hyperfine field.

To identify this state, NMR spectra are taken for single NV centers with nitrogen isotopes ^{14}N ($I = 1$) and ^{15}N ($I = 1/2$) by performing the following sequence: (1) QND nuclear spin state initialization into $m_I = 0$ (^{14}N) or $m_I = +1/2$ (^{15}N), (2) nuclear spin π -pulse and (3) QND nuclear spin readout (see fig. 1(b)). This procedure is repeated for a range of NMR frequencies and results in the spectra shown in figure 1(c). They show strong lines corresponding to nuclear spin flips of the NV^- defect in its $m_S = 0$ state (two lines for ^{14}N and a single line for ^{15}N). Additionally, weaker lines are observed (marked by arrows) that belong to the unknown state. From their spectral position and their dependence on magnetic field the nuclear spin energy level diagram in the unknown state can be deduced (fig.1(d)). This reveals hyperfine (hf) coupling to an electronic magnetic moment M which

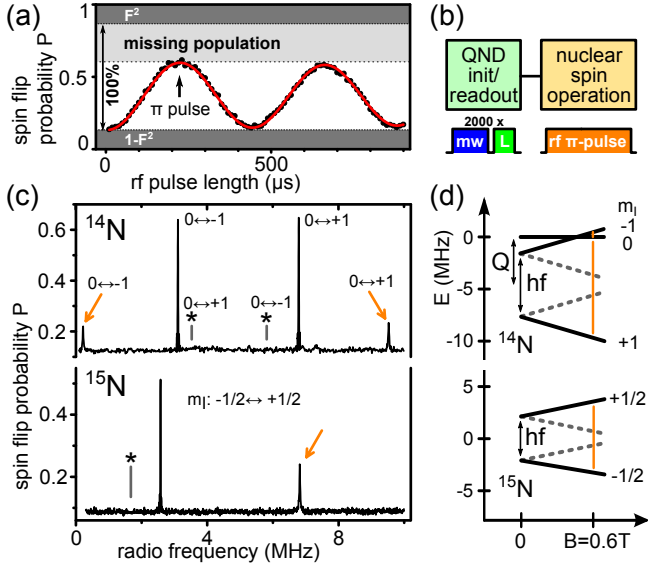


FIG. 1. (a) Nitrogen nuclear spin Rabi oscillation (NV^- , $m_S = 0$). The fidelity F reduces the achievable contrast ($\rightarrow 100\%$ population) by the dark gray regions. The even smaller Rabi amplitude is because of some population that is not in the NV^- $m_S = 0$ state (light gray region). (b) Measurement sequence. QND measurement initializes and reads out the nuclear spin state in a single shot. The green laser has a wavelength of 532 nm. An rf π -pulse flips the nuclear spin if in resonance. (c) NMR spectra showing transition frequencies of the ^{14}N and ^{15}N nuclear spin for different NV center states. The corresponding quantum numbers m_I for each transition are given. Dark state NMR transitions are marked with orange arrows; other lines belong to the bright state $m_S = 0$. Gray lines with stars mark expected transitions in the dark state (see text). (d) Energy level scheme of NV center nuclear spin in dark state. NMR transitions among spin states are marked with orange lines (arrows in (c)). Hyperfine interaction hf and quadrupole splitting Q are marked. The gray dashed lines mark the energy levels for a reversed hyperfine field (stars in (c)).

does not match the hyperfine coupling within the $S = 1$ manifold of the NV^- ground state. In addition, we have observed that the lifetime of this unknown state is $\gg 1$ s. Hence, we conclude that this state is a ground or long living metastable state.

The hyperfine coupling constants a in the unknown state are deduced according to $hf = a \cdot m_M \cdot \Delta m_I$, where hf is the hyperfine induced frequency splitting between two nuclear spin projections ($\rightarrow \Delta m_I$) and m_M is the projection of M . For ^{15}N we find $|a_{15\text{N}} \cdot m_M| = 4.242$ MHz and for ^{14}N we find $|a_{14\text{N}} \cdot m_M| = 3.03$ MHz. In addition to hyperfine coupling, ^{14}N exhibits a quadrupole splitting between nuclear spin projection $m_I = 0$ and $m_I = \pm 1$ of $Q = -4.654$ MHz (fig.1(d)).

The values above are on the same order as for the NV^- center in its triplet ground state. It is expected that hyperfine coupling to any electron spin in the $e_{x,y}$ orbitals of the NV center would be in this range (e.g. $S = 1$

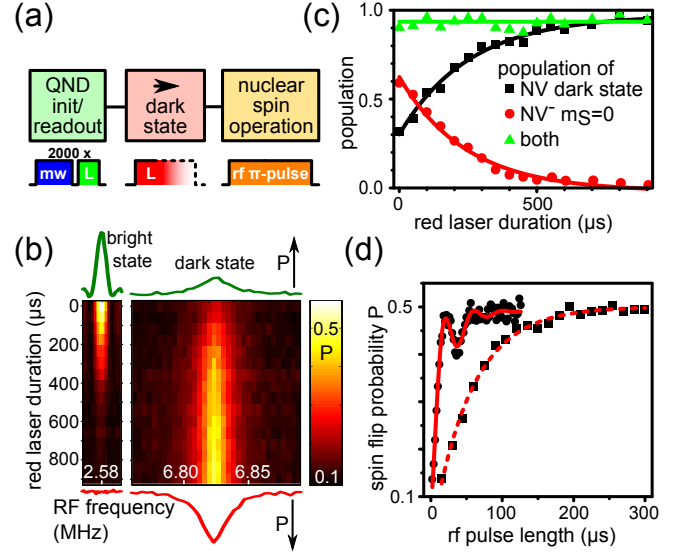


FIG. 2. (a) NMR pulse sequence to investigate transition into the dark state. After readout and initialization a red laser pulse (637 nm) of variable length transfers a certain amount of population into the dark state. A subsequent nuclear spin π -pulse monitors the NMR line intensities. (b) 2D plot of NMR amplitude (color coded) over rf frequency (horiz.) and red laser pulse length (vert.). Exemplary, the spectral regions of bright and dark state NMR lines are shown. Spectra for minimal and maximal pulse lengths are shown above and below the 2D plot. (c) Populations in the dark and bright state deduced from (b). Both populations sum up to almost 100%. (d) Nuclear spin Rabi oscillation in the dark state for rf fields of two different strengths.

of NV^- or $S = 1/2$ of NV^0 [20, 21]). Hence, the unknown state might be another charge state of the NV center exhibiting an electron spin (e.g. in addition NV^{2-} ($S = 1/2$) and NV^{2+} ($S = 1/2$)). We see indeed NMR lines for the unknown state that are commensurable with $M = S = 1/2$ (i.e. 4 NMR lines for ^{14}N and 2 lines for ^{15}N marked by arrows or stars in figure 1(c)). However, for a magnetic field of ≈ 0.6 T only two lines in the case of ^{14}N and one line for ^{15}N are visible (arrows, $m_M = \mu$) and the others are missing (stars, $m_M = -\mu$). Their absence might be due to a polarized magnetic moment into $m_M = \mu$ occurring at this magnetic field.

The interconversion between the different states of the NV center observed above can be controlled by intensity and wavelength of the applied laser radiation. As can be seen green laser light (532 nm) establishes an equilibrium between the NV^- $m_S = 0$ state and the unknown state 1(c). Now we show that the unknown state is in fact the dark state observed in [18]. It can be selectively populated by red laser illumination. Therefore, the NMR transitions of the ^{15}N nuclear spin (see fig. 1(c)) are monitored for an increasing length of the red laser (637 nm) pulses (i.e. for an increasing fraction of population in the dark state). The corresponding measurement

sequence is displayed in figure 2(a) and the results in figure 2(b). It reveals that the NMR line corresponding to the bright state vanishes completely for increasing laser pulse length whereas the NMR line corresponding to the dark state starts with a finite amplitude and rises to a maximum. From the example NMR line plots it is also visible that, whereas the bright state line shows the typical Fourier limited lineshape due to the rectangular rf π -pulse the dark state line is a much broader Lorentzian (full width at half maximum ≈ 33 kHz). In addition the nuclear spin lifetime T_1 is shorter in the dark than in the bright state ($80\text{ms} < 800\text{ms}$). Coherent driving of the dark state NMR transition reveals fast decaying Rabi oscillations (fig.3(d)) towards 50% of the initial amplitude. Thus, the amplitude in the dark state NMR lines in fig. 1(c) represent only half of the population in the dark state. From these results we can deduce the population in the NV center states for each laser pulse length (see figure 2(c)). Apparently, almost 100% of the population is distributed among the bright state's $m_S = 0$ sublevel and the dark state's $m_M = \mu$ sublevel. Furthermore, the red laser pulse transfers 100% of the population into that m_M level of the dark state.

Further inside in the nature of the dark state can be deduced from purely optical experiments. In the following, we investigate the kinetics of the optically induced transitions between dark and bright state (fig.3(a)). The quadratic dependence of the transition rates on the laser power for both directions indicates a two-photon nature of the processes (fig.3(c)). However, for stronger laser powers the dependence becomes linear which corresponds to a transition via a real excited state level that becomes saturated at higher powers. Further evidence for an excited state assisted transition to the dark state can be found by changing the steady state population of the excited state while leaving the laser intensity constant. This can be achieved by application of a misaligned magnetic field shelving the population from the excited state triplet into the metastable singlet state [23]. As expected, the transfer rate to the dark state is reduced when the magnetic field is misaligned (fig.3(b)). Another hint that we substantially populate the excited state triplet of NV^- is its electron spin polarization into $m_S = 0$ by optical excitation with the red laser. This usually works by intersystem crossing from the excited state triplet into the singlet states (fig.3(a)). The excited state of the NV^- defect is located ≈ 0.6 eV below the conduction band of bulk diamond [24]. Thus, the excited state absorption is likely to ionize the defect leading to NV^0 .

Summarizing, QND measurement enables the investigation of different NV center charge states. Using laser light of 532 nm and 637 nm we were able to selectively address different charge states. The magnetic moment M of the dark state originates from either an electron spin or an orbital angular momentum of the NV center. The position of the dark state NMR lines were identical for

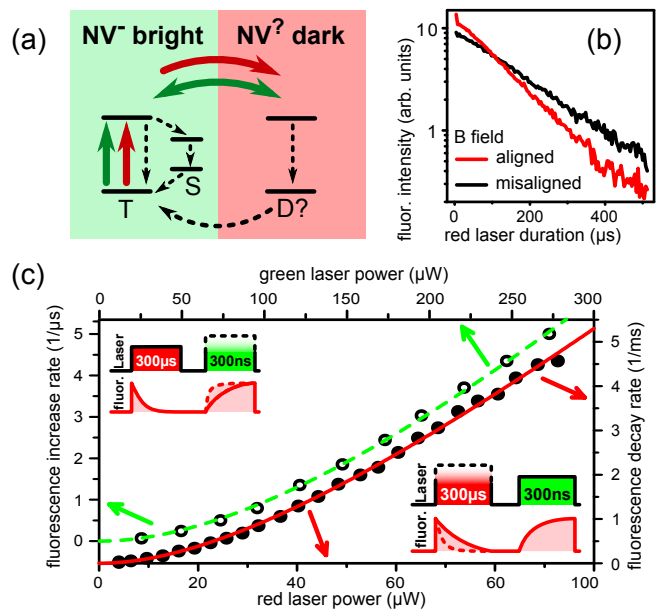


FIG. 3. (a) Energy level scheme of bright and dark state. The bright state comprises of the triple (T) and singlet (S) levels of NV^- [22] whereas the dark state is at least a doublet (D) supposedly in another charge state. The arrows symbolize transition rates, where green and red are due to the respective lasers and the black dashed arrows are decay processes. (b) The fluorescence signal of the bright state for increasing red laser duration shows an exponential decay. The decay time τ depends on the electron spin state which is influenced by aligning or misaligning the magnetic field ($m_S = 0 \rightarrow \tau = 120 \mu\text{s}$, $m_S \neq 0 \rightarrow \tau = 184 \mu\text{s}$). (c) Fluorescence decrease and increase rates depending on corresponding red or green laser power for pumping into or out of the dark state respectively. Insets show respective pulse sequences and corresponding fluorescence intensities. For fits see text.

different NV centers even in nano diamonds where strain is particularly high. Thus the nature of the magnetic moment M is very likely related to an electron spin as orbital angular momentum is very strain sensitive. Furthermore, it is known that the dynamic Jahn-Teller effect (DJT) in the NV center can average out orbital angular momentum at room temperature as shown for the NV^- excited state [25]. In addition, it is supposed to cause EPR line broadening in the NV^0 $S = 1/2$ ground state [21, 26] and can therefore be responsible for the observed fast dephasing of the nuclear spin in our experiments. All observations presented in this letter are in agreement with the assignment of the dark state to the NV^0 center.

All this sheds new light on previous experiments using single NV^- centers. Previous spin operations have been only 70% efficient (i.e. only if the NV resides in the bright state). Surprisingly, QND initialization and readout of single nuclear spins is working even under this condition showing that the nuclear spin state is preserved during ionization and deionization. Our results also make 70% an upper bound on the fluorescence quantum yield

of the investigated NV centers upon green illumination (not taking into account intersystem crossing that would further decrease the quantum yield). If there is a way to bring 100% of the population into the bright state, NV⁻ spin operations will be 100% efficient. This is of prime importance for numerous emerging applications of the NV defect center [1–6, 8, 10, 11]. An alternative route to go is using the nuclear spin in the dark state as a qubit. It is possible to initialize it to 100% and single shot read-out is working as well via the bright state. To improve quantum state lifetimes the application of uniaxial stress might be successful in case of DJT [21].

We thank Roman Kolesov for experimental assistance and discussion as well as Petr Siyushev and Gopalakrishnan Balasubramanian for discussion.

* p.neumann@physik.uni-stuttgart.de

† Research Institute for Solid State Physics and Optics, Hungarian Academy of Sciences, 1525 Budapest, Hungary

- [1] F. Jelezko, T. Gaebel, I. Popa, M. Domhan, A. Gruber, and J. Wrachtrup, *Physical Review Letters* **93**, 130501 (2004).
- [2] L. Childress, M. V. G. Dutt, J. M. Taylor, A. S. Zibrov, F. Jelezko, J. Wrachtrup, P. R. Hemmer, and M. D. Lukin, *Science* **314**, 281 (2006).
- [3] T. Gaebel, M. Domhan, I. Popa, C. Wittmann, P. Neumann, F. Jelezko, J. R. Rabeau, N. Stavrias, A. D. Greentree, S. Praver, J. Meijer, J. Twamley, P. R. Hemmer, and J. Wrachtrup, *Nature Physics* **2**, 408 (2006).
- [4] M. V. G. Dutt, L. Childress, L. Jiang, E. Togan, J. Maze, F. Jelezko, A. S. Zibrov, P. R. Hemmer, and M. D. Lukin, *Science* **316**, 1312 (2007).
- [5] P. Neumann, N. Mizuochi, F. Rempp, P. Hemmer, H. Watanabe, S. Yamasaki, V. Jacques, T. Gaebel, F. Jelezko, and J. Wrachtrup, *Science* **320**, 1326 (2008).
- [6] P. Cappellaro, L. Jiang, J. S. Hodges, and M. D. Lukin, *Physical Review Letters* **102**, 210502 (2009).
- [7] G. D. Fuchs, V. V. Dobrovitski, D. M. Toyli, F. J. Heremans, and D. D. Awschalom, *Science* **326**, 1520 (2009).
- [8] P. Neumann, R. Kolesov, B. Naydenov, J. Beck, F. Rempp, M. Steiner, V. Jacques, G. Balasubramanian, M. L. Markham, D. J. Twitchen, S. Pezzagna, J. Meijer, J. Twamley, F. Jelezko, and J. Wrachtrup, *Nat Phys* **6**, 249 (2010).
- [9] D. M. Toyli, C. D. Weis, G. D. Fuchs, T. Schenkel, and D. D. Awschalom, *Nano Lett* **10**, 3168 (2010).
- [10] G. Balasubramanian, I. Y. Chan, R. Kolesov, M. Al-Hmoud, J. Tisler, C. Shin, C. Kim, A. Wojcik, P. R. Hemmer, A. Krueger, T. Hanke, A. Leitenstorfer, R. Bratschkitsch, F. Jelezko, and J. Wrachtrup, *Nature* **455**, 648 (2008).
- [11] J. R. Maze, P. L. Stanwix, J. S. Hodges, S. Hong, J. M. Taylor, P. Cappellaro, L. Jiang, M. V. G. Dutt, E. Togan, A. S. Zibrov, A. Yacoby, R. L. Walsworth, and M. D. Lukin, *Nature* **455**, 644 (2008).
- [12] A. Gruber, A. Drabenstedt, C. Tietz, L. Fleury, J. Wrachtrup, and C. vonBorczykowski, *Science* **276**, 2012 (1997).
- [13] G. Balasubramanian, P. Neumann, D. Twitchen, M. Markham, R. Kolesov, N. Mizuochi, J. Isoya, J. Achard, J. Beck, J. Tisler, V. Jacques, P. R. Hemmer, F. Jelezko, and J. Wrachtrup, *Nat Mater* **8**, 383 (2009), 1476-1122 10.1038/nmat2420 10.1038/nmat2420.
- [14] G. de Lange, Z. H. Wang, D. Rist, V. V. Dobrovitski, and R. Hanson, *Science* **330**, 60 (2010).
- [15] L. Rondin, G. Dantelle, A. Slablab, F. Grosshans, F. Treussart, P. Bergonzo, S. Perruchas, T. Gacoin, M. Chaigneau, H.-C. Chang, V. Jacques, and J.-F. Roch, *Phys. Rev. B* **82**, 115449 (2010).
- [16] N. B. Manson and J. Harrison, *Diamond & Related Materials* **14**, 1705 (2005).
- [17] T. Gaebel, M. Domhan, C. Wittmann, I. Popa, F. Jelezko, J. R. Rabeau, A. D. Greentree, S. Praver, E. Trajkov, P. Hemmer, and J. Wrachtrup, *Applied Physics B* **82**, 243 (2006).
- [18] K. Y. Han, S. K. Kim, C. Eggeling, and S. W. Hell, *Nano Letters* **10**, 3199 (2010), <http://pubs.acs.org/doi/pdf/10.1021/nl102156m>.
- [19] P. Neumann, J. Beck, M. Steiner, F. Rempp, H. Fedder, P. R. Hemmer, J. Wrachtrup, and F. Jelezko, *Science* **329**, 542 (2010), <http://www.sciencemag.org/cgi/reprint/329/5991/542.pdf>.
- [20] S. Felton, A. M. Edmonds, M. E. Newton, P. M. Martineau, D. Fisher, D. J. Twitchen, and J. M. Baker, *Phys. Rev. B* **79**, 075203 (2009).
- [21] S. Felton, A. Edmonds, M. Newton, P. Martineau, D. Fisher, and D. Twitchen, *Phys. Rev. B* **77**, 081201 (2008).
- [22] V. M. Acosta, A. Jarmola, E. Bauch, and D. Budker, *Phys. Rev. B* **82**, 201202 (2010).
- [23] R. J. Epstein, F. M. Mendoza, Y. K. Kato, and D. D. Awschalom, *Nature Physics* **1**, 94 (2005).
- [24] J. W. Steeds, S. J. Charles, J. Davies, and I. Griffin, *Diamond and Related Materials* **9**, 397 (2000).
- [25] K.-M. C. Fu, C. Santori, P. E. Barclay, L. J. Rogers, N. B. Manson, and R. G. Beausoleil, *Phys. Rev. Lett.* **103**, 256404 (2009).
- [26] A. Gali, *Physical Review B* **79**, 235210 (2009).